Received: 14 June 2022 | Revised: 29 December 2022 | Accepted: 1 January 2023

DOI: 10.1002/rra.4106

RESEARCH ARTICLE

WILEY

Investigation of stage-discharge model performance for streamflow estimating: A case study of the Gono River, Japan

Mahmoud F. Maghrebi[1] | Sajjad M. Vatanchi[1] | Kiyosi Kawanisi[2]

[1]Civil Engineering Department, Ferdowsi University of Mashhad, Mashhad, Iran

[2]Department of Civil and Environmental Engineering, Graduate School of Engineering, Hiroshima University, Higashihiroshima, Japan

Correspondence
Mahmoud F. Maghrebi, Civil Engineering Department, Ferdowsi University of Mashhad, Mashhad, Iran.
Email: maghrebi@um.ac.ir

Abstract

In water resource studies, long-term measurements of river streamflow are essential. They allow us to observe trends and natural cycles and are prerequisites for hydraulic and hydrology models. This paper presents a new application of the stage-discharge rating curve model introduced by Maghrebi et al. (2016) to estimate continuous streamflow along the Gono River, Japan. The proposed method, named single stage-discharge (SSD) method, needs only one observed data to estimate the continuous streamflow. However, other similar methods require more than one observational data to fit the curve. The results of the discharge estimation by the SSD are compared with the improved fluvial acoustic tomography system (FATS), conventional rating curve (RC), and flow-area rating curve (FARC). Some statistical indicators, such as the coefficient of determination (R^2), root mean square error (RMSE), percent bias (PBAIS), mean absolute error (MAE), and Kling-Gupta efficiency (KGE), are used to assess the performance of the proposed model. ADCP data are used as a benchmark for comparing four studied models. As a result of the comparison, the SSD method outperformed of FATS method. Also, the three studied RC methods were highly accurate at estimating streamflow if all observed data were used in calibration. However, if the observed data in calibration was reduced, the SSD method by $R^2 = 0.99$, RMSE = 2.83 (m^3/s), PBIAS = 0.715(%), MAE = 2.30 (m^3/s), and KGE = 0.972 showed the best performance compared to other methods. It can be summarized that the SSD method is the feasible method in the data-scarce region and delivers a strong potential for streamflow estimation.

KEYWORDS
continuous streamflow, model performance, river discharge, stage-discharge rating curve, streamflow measurements

1 | INTRODUCTION

In river management, obtaining continuous streamflow estimation is critical since extremely high flows can cause erosion and flood damage (Muste, Ho, & Kim, 2011). Shallow flows, on the other hand, can affect water quality, harm fish, and reduce human access to water. Moreover, hydrological models need accurate river flow data to improve and provide credible predictions. As a result, it is crucial to establish a method or technology for measuring or estimating discharge. The stage-discharge rating curve is a simple and common indirect river flow estimation method (Ocio, Le Vine, Westerberg, Pappenberger, & Buytaert, 2017). This method can estimate the discharge at high levels using low-level data (especially in poorly gauged catchments). Rating curves are recommended because direct measurements of high flows are complicated and costly (Clarke, 1999). Among the different methods for estimating rating curves, the method with the most accuracy and the least need for observational data is more valuable.

Several devices that aid in measuring continuous velocity and discharge have been adopted, namely acoustic/ultrasonic velocity meters (AVMs/UVMs) and horizontal acoustic Doppler current profilers (H-ADCPs). AVMs/UVMs, based on the travel time method, can produce accurate mean velocity measurements along diagonally crossing pathways in a channel (Kawanisi, Razaz, Ishikawa, Yano, & Soltaniasl, 2012). Also, H-ADCPs are increasingly being established for continuous river monitoring (Cheng et al., 2019). The accuracy of velocities and discharges given by the H-ADCP placed at the Saint-Georges gauging station was evaluated in the field by Le Coz, Pierrefeu, and Paquier (2008). In that study, comparing the H-ADCP velocity measurements with ADCP data indicated that the measures were only reliable at near-field distances (60 m out of a 95 m section width). ADCPs are acoustic instruments that measure the velocity by the reflection of the sound of a moving particle with a current (Gordon, 1989).

Improved streamflow measurements have resulted from the development of various techniques. For example, Kawanisi et al. (2012) used the fluvial acoustic tomography system (FATS). This innovative system can detect cross-sectional average velocity and discharges with high frequency to take long-term observations in a mountainous river. FATS uses the same fundamental principle as AVMs, based on the "time-of-travel" method. The acoustic signals of FATS are transmitted via omnidirectional transducers at 10–55 kHz, with a reciprocal sound transfer between two acoustic stations located on either side of the river (Kawanisi, Al Sawaf, & Danial, 2018). FATS, which consists of a pair of transducers, is a low-cost device that can measure cross-sectional average velocity without requiring complex postprocessing.

Establishing a stage-discharge relationship (rating curve, e.g., Herschy, 2009) to convert continuously recorded water levels into discharge time series is the most popular and easiest way of monitoring streamflow at a gauging station. The power function is a unique function commonly utilized as a rating curve in river hydraulics (e.g., Di Baldassarre & Montanari, 2009). It should be noted that this approach is only viable if the flow is steady; for unstable flows, which are common in natural streams, this approach is unsatisfactory and introduces a significant source of errors.

There are several methods for establishing a rating curve. For example, Manfreda et al. (2020) proposed a new method to exploit cross-sectional geometry to derive more robust flow rating curves. Flow velocity and wetted cross-section functions are used in the proposed procedure to estimate flow rating curves. This method may be suitable as an alternative to the conventional method of determining rating curves. The results showed that the new approach becomes advantageous with limited observations.

Studies have been conducted on estimating the stage-discharge rating curve through data-driven and machine-learning methods. For example, Sivapragasam and Muttil (2005) suggested using a support vector machine (SVM) to extrapolate rating curves. They showed that SVM is better suited for extrapolation than artificial neural networks (ANNs). Bhattacharya and Solomatine (2000) used ANNs widely used in various water-related research areas to define stage-discharge relations. They demonstrated that using ANN is superior to the conventional statistical stage-discharge model. Ghorbani, Khatibi, Goel, FazeliFard, and Azani (2016) examined the performance of SVM, ANN, RC, and multiple linear regressions (MLR) in estimating river discharge time series. Various performance measures have been used to evaluate the results, indicating that SVM and ANN perform better than conventional RC and MLR models. Compared to RC and MLR, SVM and ANN predict peak values with greater reliability. In practice, however, these conventional models perform well for many problems.

The utility of the fuzzy neural network modeling method in determining the stage-discharge relationship was investigated by Deka and Chandramouli (2003). They also showed that the fuzzy neural network model's performances were better than the neural network model and conventional rating curve approach. Shukla et al. (2022) evaluated adaptive neuro-fuzzy inference systems (ANFIS), ANN, and wavelet-based artificial neural networks (WANN) for estimating discharge. They found that ANFIS outperformed ANN- and WANN-based discharge estimation models. All the papers that used machine learning methods needed a lot of measured discharge data to model the rating curve. Therefore, in this paper, these methods are not used because they are not feasible in data-scarce regions.

A model that could estimate the stage-discharge rating curve in open channels and rivers was proposed by Maghrebi, Ahmadi, Attari, and Maghrebi (2016). In this method, each water stage and discharge pair is considered the reference data for generating the entire stage-discharge relationship in any desired water depth. In addition, having geometrical and hydraulic data at different levels is necessary for estimating the rating curve. Here hydraulic and statistical methods are applied simultaneously.

This study investigates a new application of the stage-discharge rating curve (SSD) method, introduced by Farsoudeh and Maghrebi (2018), for continuous flow estimation. This study was carried out in the Gono River, Japan. This research aims to evaluate the performance of the proposed stage-discharge rating curve for estimating continuous streamflow. Some statistical measures, including R^2 (coefficient of determination), root mean square error (RMSE), percent bias (PBIAS), mean absolute error (MAE), and Kling-Gupta efficiency (KGE), have been used to evaluate the performance of the SSD. The proposed model is further evaluated compared to the FATS, power function rating curves (RC), and flow-area rating curve (FARC).

2 | MATERIALS AND METHODS

2.1 | Study area

The Gono River survey site is in Miyoshi City, Japan (see Figure 1). The confluence of the Basen and Saijo rivers forms the Gono River. The observation site is about 3.6 km downstream of the river confluences. The river is 115 m wide, and the slope of the bed near the observation site is 0.11%, with a Manning roughness of 0.03 based on the water surface profile (Al Sawaf, Kawanisi, Kagami, Bahreinimotlagh, & Danial, 2017).

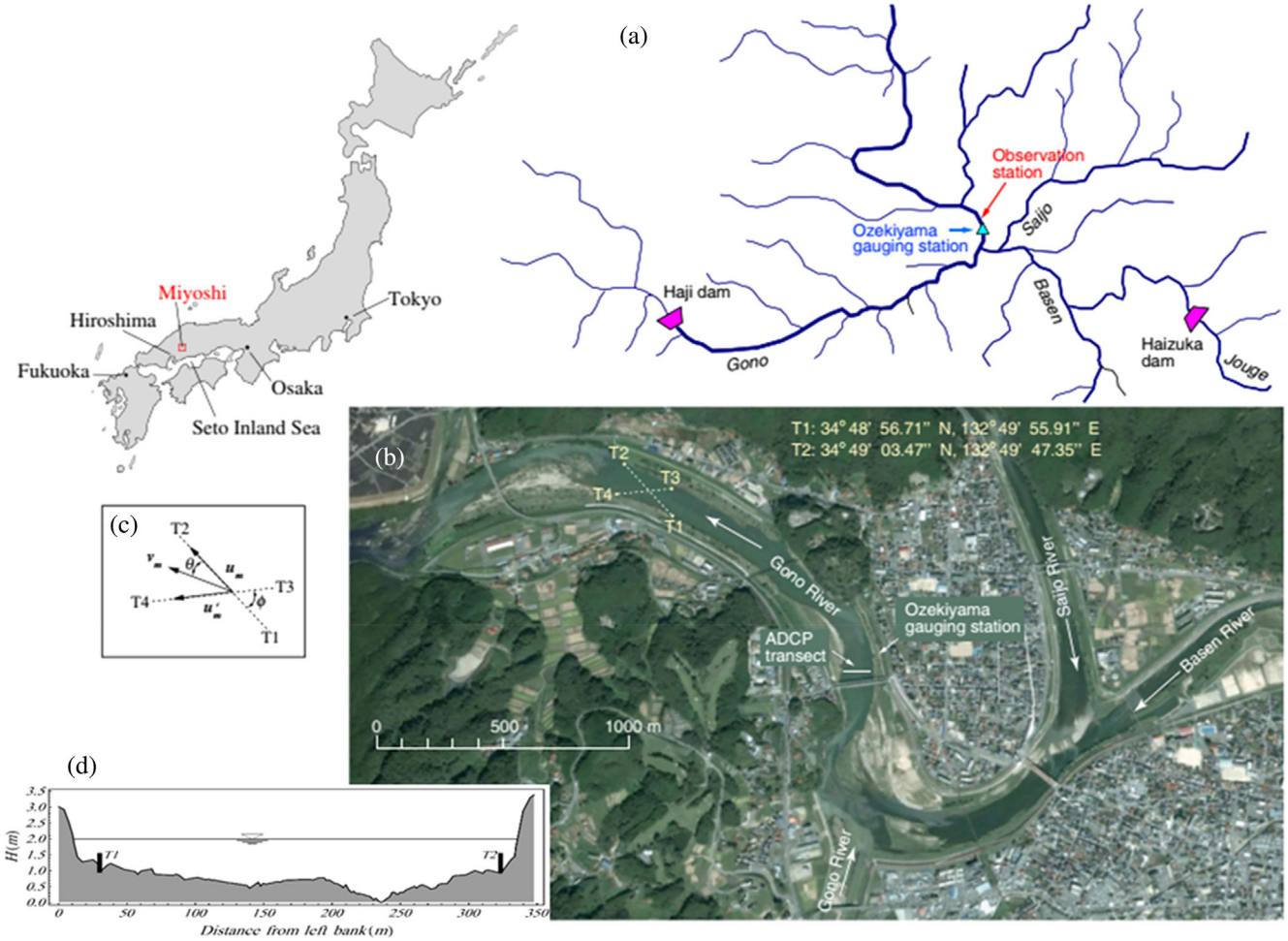

FIGURE 1 Study area and experimental site: (a) map of the river network; (b) the location map shows the position of the transducers, the acoustic Doppler current profiler transect, and the Ozekiyama gauging station; (c) stream velocity vector configuration; (d) studied cross-section. *H* denotes height (stage) in m (Kawanisi et al., 2018) [Color figure can be viewed at wileyonlinelibrary.com]

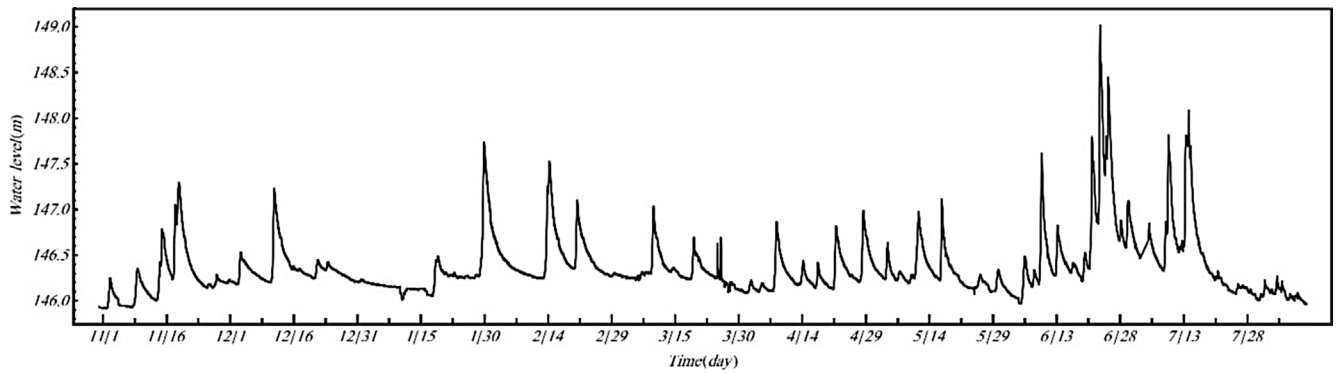

FIGURE 2 Water level data from October 30, 2015 to August 10, 2016

2.2 | Water level measurement

HOBO U20 temperature-depth loggers were mounted to the two transducers and used to measure the water level and temperatures (Kawanisi et al., 2018). Streamflow was estimated using the cross-sectional average velocity and water level data. The processing unit was connected to the internet to read data in real time.

Figure 2 shows the water level data between October 30, 2015 and August 10, 2016 to estimate the hydrograph. Submersible level transmitters collected water levels every 30 s (Acculevel ACL-10-A; Keller America; Kawanisi et al., 2018).

2.3 | ADCP streamflow measurements

Streamflow data were collected utilizing a moving-boat ADCP from July 2015 to March 2016 to get the measured discharge data. Two to four transects were used to estimate each streamflow. ADCP measurements were performed using a Workhorse Monitor ADCP (1,228.8 kHz) or a Teledyne RDI (Poway, California) StreamPro ADCP (2,457.6 kHz). In shallow water, the StreamPro ADCP was deployed; the depth of the cells was 0.1 m, and the depth of the first cell was 0.19 m. The Workhorse Monitor ADCP was set up with a 0.25 m cell size and a 0.68 m initial cell depth.

2.4 | Continuous streamflow measurement by FATS

With the newly improved FATS frameworks, two precise timing signals are provided by GPS receivers. A timing pulse (1 Hz) ensures that two frameworks run simultaneously. Another 10 MHz signals is employed as the FATS base clock to transmit and receive high-precision signals, which possess long-term frequency accuracy and stability. These enhancements make the prior FATS system more reliable and run for extended periods. Obtaining automatic real-time data flow has been made easier by integrating an automatic data transfer function and an Internet connection (Kawanisi et al., 2018). The FATS processing unit is also connected to water level sensors to estimate the cross-section of the flow. As a result, flow data can be recorded for long periods with high time resolution (at regular intervals).

Kawanisi et al. (2018) demonstrated that FATS is a practical and powerful approach to measuring continuous streamflow at high-frequency levels. Their paper introduced improved FATS, a method that can be used to automatically measure streamflow for a long period with high temporal resolution. Finally, with decreasing water depth, the relative error in the FATS increased, and the highest error under low-flow conditions was 14%. An advanced application of FATS involves deploying an array of acoustic stations using different M-sequence codes and reconstructing a depth-averaged flow velocity distribution pattern (Razaz, Kawanisi, Kaneko, & Nistor, 2015).

A geometry view of the Gono River is shown in Figure 1d, along with two omnidirectional transducers (T1 and T2). On December 25, 2015, the bed level between the two transducers was measured by an autonomous unmanned boat using a single-beam echo sounder and GPS. Although the cross-section along the transmission line is oblique, different from that in usual discharge measurements, no further correction is required. The choice of these sections results in a lower error in discharge estimation because the distance is much longer and the flow velocity component along the sonar ray is smaller, so the accuracy of measurement and estimations is increased. A slight deviation in real-time results in a lower error rate when dealing with large distances. Using a section perpendicular to the flow direction is not possible in the FATS technique.

Continuous streamflow measurements were carried out using FATS from October 30, 2015 to August 10, 2016. The Gono River was crossed diagonally by two omnidirectional broadband transducers (T1 and T2), as shown in Figure 1. The distance between these transducers was 294 m. Both transducers transmitted the acoustic pulses simultaneously every 30 s. The streamflow Q is calculated as follows:

$$Q = A(H)\tan\theta \times u_m, \tag{1}$$

where $A(H)$ is the cross-sectional area along the transmission line of T1–T2 and is obtained from a stage-area relation, H is the stage, u_m is the section-averaged velocity along the acoustic path, and θ is the flow angle. As seen in Figure 1b, the angle between the ray path and the streamline is θ. The average value of θ was approximately 15.2° (Kawanisi, Bahrainimotlagh, Al Sawaf, & Razaz, 2016). Although the actual cross-sectional area increased beyond the two transducers, it can be seen from Figure 1b that the area out of the transducers is covered with submerged weeds, algae, and moss. Hence, their contribution to discharge conveyance through these areas is very much limited. Acoustic data were collected on both sides of the river and then transferred to a processing unit, where average velocities were computed automatically.

2.5 | Conventional RC

A stage-discharge rating curve describes a relationship between the water level (stage) of a channel cross-section and the discharge at that section (Herschy, 2009). As a result, it reduces the cost and time associated with taking discharge measurements. If the discharge values are plotted against the stages, a relationship represents the effects of various channel parameters and flows (Ajmera & Goyal, 2012). The power function is a simple model extensively used as a rating curve in river hydraulics (with specific physical justifications):

$$Q = c_1(h - c_2)^{c_3}, \tag{2}$$

where Q is discharge, c_1, c_2, and c_3 are calibration constants and h is the water stage. The constants were estimated using the least-squares method. In this method, at least three measured discharge data are required.

2.6 | Flow-area rating curve

Basic streamflow monitoring involves measuring the average flow velocity (V), typically with several distributed point measurements, and evaluating the associated cross-sectional wetted area (A). Using both datasets and using the averaged flow velocity as a regression function, Manfreda (2018) proposes that the rating curve can be determined as follows:

$$Q = V(H) \times A(H). \tag{3}$$

In the equation, V and A represent the relationship between mean flow velocity and wetted area as a function of depth (H). These

functions can be fitted using existing observations and field surveys. The flow-area model calibrates the above functions separately and then multiplies them to obtain the discharge. The geometric relationship can be obtained using topographic surveys. Recent advances in topographic surveys, such as modern portable GPS, laser scanners, and photogrammetry, can be helpful for this method (Manfreda et al., 2020).

2.7 | Proposed stage-discharge model

This study introduces a new method for estimating the rating curve that uses hydraulic parameters and only one pair of measured discharge and stage data as calibration. Although this method is more complicated than the power function, managers and decision-makers can use it in areas lacking measured data because only one measured discharge data for calibration is needed. Because of this, the method is called single stage-discharge (SSD) method. In other words, measuring low-flow (low water level) data as a reference point makes it possible to estimate the high flow. The proposed method cannot be used in ungauged basins since at least one observational data is required. The following is how to extract the SSD model.

According to Farsoudeh and Maghrebi (2018), the discharge is a function of the following parameters at any water level in the channel:

$$Q = A^{a_1} P^{a_2} P_t^{a_3} U_{SPM}^{a_4} n^{a_5} S_0^{a_6}, \tag{4}$$

where Q is the discharge, A is the cross-sectional area, P is the wetted perimeter of the flow section, P_t is the sum of P and the width (T) of the water surface ($P_t = P + T$), n is the Manning roughness, S_0 is the bed slope, and U_{SPM} is the cross-sectional mean flow velocity in the streamwise direction, introduced by Maghrebi (2006). a_1 to a_6 are the calibration parameters.

In the field of hydraulics, Maghrebi (2006) utilized the Biot–Savart law to quantify the impact of the wetted perimeter on the velocity at any point on the channel cross-section. A triangular mesh was first placed on the cross-section of the channel, as shown in Figure 3, to determine isovel contours. The wetted perimeter was then split into infinitesimal components ds, and the impact of ds on the velocity du at the triangle element's centroid was determined as follows:

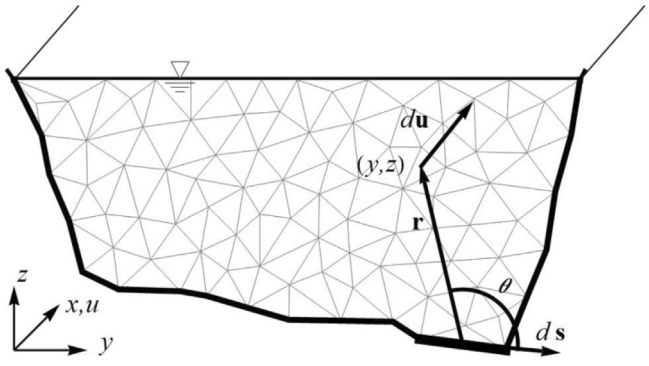

FIGURE 3 Effect of boundary elements on an arbitrary point at the cross-section

$$du = f(r) \times c_1\, ds, \tag{5}$$

where c_1 is a boundary roughness-dependent constant, du is velocity deviation, and $f(r)$ is the velocity function. Maghrebi and Ball (2006) recommend a seventh root power-law relationship for a natural river's velocity function. The average velocity of the cross-section (U_{SPM}) can be determined as follows:

$$U_{SPM} = \frac{\int_A \int_{boundry} c \times r^{\frac{1}{7}} \times \sin\theta\, ds\, dA}{\int_A dA}, \tag{6}$$

where c is a coefficient related to the roughness of the wall, shape, and dimensions of the cross-section, θ is the angle between r (distance from the boundary to the desired point) and ds, and dA is the area of each triangular mesh.

The general form of the relationship, according to Equation (4), is as follows:

$$\frac{Q_e}{Q_r} = \left(\frac{A_e}{A_r}\right)^{a_1} \left(\frac{P_e}{P_r}\right)^{a_2} \left(\frac{(P_t)_e}{(P_t)_r}\right)^{a_3} \left(\frac{(U_{SPM})_e}{(U_{SPM})_r}\right)^{a_4} \left(\frac{n_e}{n_r}\right)^{a_5} \left(\frac{(S_0)_e}{(S_0)_r}\right)^{a_6}. \tag{7}$$

Subscripts r and e stand for the referenced and estimated values, respectively. In Equation (7), the impact of S_0 is neglected in the computational process because of the remaining constant at all water stages. The exponent a_5 is adjusted to -1 to simplify and speed up the computations and reflect the inverse relationship between the discharge and Manning's roughness. If the Manning roughness coefficient (n) is homogeneous, the influence of n on the computing process is ignored because it is the same at all levels. It is significant to note that the U_{SPM} in Equation (7) acts as the average velocity parameter. Because of the continuity equation, its power is maintained constant, that is, $a_4 = 1$. Thus, it is only necessary to evaluate a_1, a_2, and a_3. Using the multivariate Newton method, the difference between the exact and estimated values (Q, H) is minimized to optimize the values for a_1, a_2, and a_3. The initial step in determining exponent values is to collect data from observational (measured) and theoretical (Manning's equation) rating curves for various cross-sections. The most authentic relationship, as shown by Farsoudeh and Maghrebi (2018), is related to the lowest values of the normalized root mean square error (NRMSE; Equation 8). It can be achieved by minimizing the summation of NRMSEs for both rectangular and compound channels, as specified below:

$$NRMSE = \frac{\frac{1}{N}\sum_{i=1}^{N} \sqrt{\frac{1}{N}\sum_{i=1}^{N} \left[\left(Q_r \left(\frac{A_e}{A_r}\right)^{a_1} \left(\frac{P_e}{P_r}\right)^{a_2} \left(\frac{(P_t)_e}{(P_t)_r}\right)^{a_3} \left(\frac{(U_{SPM})_e}{(U_{SPM})_r}\right)^{1}\right)_i - (Q_r)_i\right]}}{(Q_r)_{max} - (Q_r)_{min}}. \tag{8}$$

where N is the number of measured discharge data, Q_r is the observational or theoretical discharge, and Q_e is the estimated discharge. After the optimization, the final relation has been suggested by Farsoudeh and Maghrebi (2018) as follows:

$$Q_e = Q_r \left(\frac{A_e}{A_r}\right)^{0.97} \left(\frac{P_e}{P_r}\right)^{-1.27} \left(\frac{(P_t)_e}{(P_t)_r}\right)^{0.83} \left(\frac{(U_{SPM})_e}{(U_{SPM})_r}\right). \quad (9)$$

In order to estimate discharge by Equation (8), all of the effective hydro-geometric parameters are required to be calculated at all water stages. In other words, for an arbitrary open channel, one should calculate the following parameters: $A = A(H)$, $P = P(H)$, $P_t = P_t(H)$, $n = n(H)$, and $U_{SPM} = U_{SPM}(H)$. Furthermore, only one pair of measured discharge and stage data is required to estimate the entire rating curve. In general, the following steps should be followed to obtain the stage-discharge rating curves:

1. The single measured discharge (reference point) is known at a referenced water level, H_r. Any arbitrary measured discharge data can be from the lower, middle, or upper stages.
2. The mean cross-sectional velocity U_{SPM} is calculated at the reference level and other stages (Maghrebi, 2006).
3. Geometric parameters such as A, P, P_t, and equivalent roughness n (by the experimental equations; Vatanchi & Maghrebi, 2019) are calculated for reference and the estimated levels.
4. Discharge can be computed by replacing the predicted values in Equation (9).
5. The stage-discharge curve is generated by connecting the computed values of Q_e at various levels. Also, water level data can estimate the streamflow within the desired period. Figure 4 shows the flowchart of the proposed methodology.

As well as the homogeneous bed roughness, the steady flow condition was one of the SSD model limitations. Also, in this study, the effect of river curvature was ignored.

2.8 | Performance criteria

In order to clarification of the proposed model performance, some of the statistical measures, including the RMSE, the R^2, PBIAS, MAE, and KGE based on the estimated discharge Q_e and the measured discharge data Q_r are described as the following:

$$R^2 = \left[\frac{\sum_{i=1}^{N}\left[(Q_r)_i - \overline{(Q_r)}_i\right]\left[(Q_e)_i - \overline{(Q_e)}_i\right]}{\sqrt{\sum_{i=1}^{N}\left[(Q_r)_i - \overline{(Q_r)}_i\right]^2}\sqrt{\sum_{i=1}^{N}\left[(Q_e)_i - \overline{(Q_e)}_i\right]^2}}\right]^2, \quad (10)$$

$$\mathrm{RMSE}(\mathrm{m}^3/\mathrm{s}) = \sqrt{\frac{\sum_{i=1}^{N}\left[(Q_r)_i - (Q_e)_i\right]^2}{N}}, \quad (11)$$

$$\mathrm{PBIAS}(\%) = \frac{\sum_{i=1}^{N}\left[(Q_r)_i - (Q_e)_i\right] \times 100}{\sum_{i=1}^{N}(Q_r)_i}, \quad (12)$$

$$\mathrm{MAE}(\mathrm{m}^3/\mathrm{s}) = \frac{\sum_{i=1}^{N}|Q_p - Q_m|}{N}, \quad (13)$$

$$\mathrm{KGE} = 1 - \sqrt{(r-1)^2 + \left(\frac{\overline{Q_e}}{\overline{Q_r}} - 1\right)^2 + \left(\frac{CV_e}{CV_r}\right)^2}, \quad (14)$$

where Q_r is the measured discharge (ADCP) as reference points, and Q_e is the estimated discharge by the proposed model, FATS, RC, and flow area. $\overline{Q_r}$ and $\overline{Q_e}$ are the mean measured and estimated discharge, respectively. r is the correlation coefficient, and CV is the coefficient of variation.

The square root of the average square of all of the errors is called RMSE (Elbeltagi et al., 2022). As a scalar-dependent measure of accuracy, RMSE can only compare prediction errors between models or variables and not between two different variables (Singh et al., 2022). RMSE lies between 0 to ∞.

R^2 help to determine whether the estimated and observed data are associated statistically (collinearity; Singh et al., 2022). In statistics, R^2 refers to the ratio of explained variation to total variation. Values

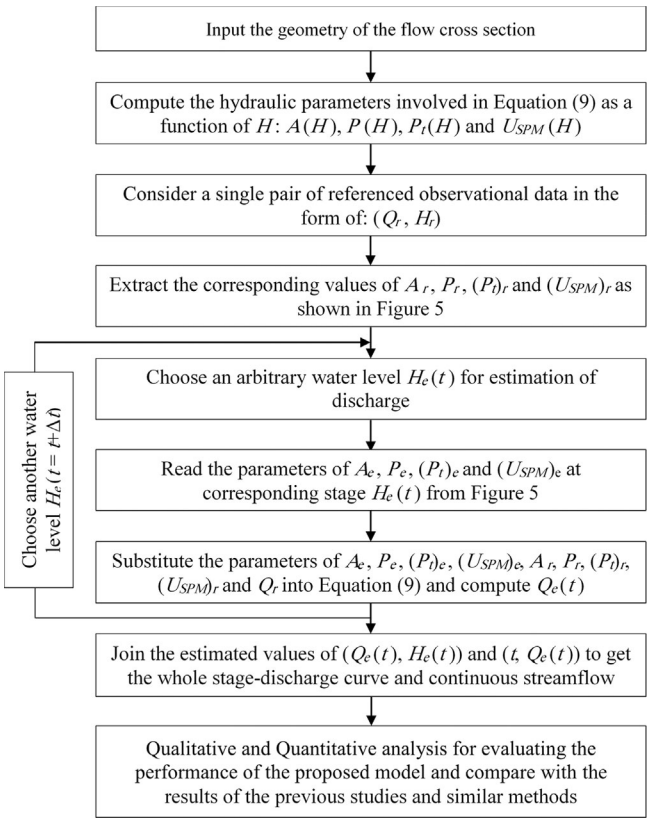

FIGURE 4 Flowchart of methodology

of 0.5 or greater are generally considered acceptable; the higher the value, the less error variance (Singh et al., 2022). It is sensitive to outliers and insensitive to additive and proportional differences between observed and estimated data (Singh et al., 2022).

The optimal value of PBIAS, expressed as a percentage, is 0.0, which indicates an accurate model. In the model, positive values indicate underestimation bias, while negative values indicate overestimation bias (Gupta, Sorooshian, & Yapo, 1999). In PBIAS, it is determined whether the observed data is larger or smaller than the estimated data; it measures the average tendency of observed data to differ from estimated data (Gupta et al., 1999). Data deviations are reported as a percentage by PBIAS after they have been evaluated.

In MAE, errors are measured only in magnitude, without consideration of their direction. The accuracy of a model increases with decreasing MAE. High errors caused by outliers are not penalized by MAE (Chicco, Warrens, & Jurman, 2021). Sometimes the significant errors coming from the outliers are treated the same as low errors.

KGE (Gupta, Kling, Yilmaz, & Martinez, 2009) is based on a decomposition of NSE into its constitutive components (correlation, variability bias, and mean bias) and addresses several perceived shortcomings in NSE. It is increasingly used for model calibration and evaluation (Liu, 2020). KGE = 1 indicates perfect agreement between estimations and observations, and negative KGE values indicate poor model performance (Knoben, Freer, & Woods, 2019).

A model with a higher R^2 and KGE value and lower RMSE, PBAIS, and MAE values decree a relatively better model for streamflow estimation (Vishwakarma et al., 2022).

3 | RESULTS AND DISCUSSION

This section deals with the development and results of the Gono River's SSD, FATS, RC, and FARC methods. The qualitative performance evaluation of the models was achieved by visual observations such as time series and box plots, and quantitative assessments were carried out using different statistical and hydrological performance indices.

3.1 | The application of the proposed model (SSD) in continuous streamflow

The parameters in Equation (9) have to be estimated by exploiting the information coming from the knowledge of the cross-section (Figure 1d). In Figure 5a, the variation of these parameters is shown. The values of A_{max}, P_{max}, $(P_t)_{max}$, and $(U_{SPM})_{max}$ are the maximum values of these parameters at the maximum stage (H_{max}). In the Gono River, the maximum value of the stage based on the measured stage data is $H_{max} = 3$ m. The values of A_{max}, P_{max}, $(P_t)_{max}$, and $(U_{SPM})_{max}$ are 737 m^2, 341 m, 682 m, and 30 m/s, respectively. Therefore, A, P, P_t, and U_{SPM} can be calculated at any arbitrary stage. In Figure 5a, the diagrams for P and P_t do not coincide, and a slight difference exists.

Therefore, the stage-discharge rating curve can be plotted using efficient parameters and Equation (9). As shown in Figure 5b, the proposed rating curve has been estimated based on three different and arbitrary reference points to show the performance of the model in three different stages. It should be mentioned that only one reference point is needed in this model.

In the next step, by considering the measured discharge at each stage and time as a reference point on the streamflow and its related effective parameters, discharges at other levels and times can be calculated using Equation (9). Our intention is to estimate streamflow using only one measured discharge (reference point) at a given stage and time. The desired reference points are selected, that is, P1, P5, and P10, to evaluate the performance of the model at different stages. Figure 6 shows the Gono River hydrograph based on three desired reference points from (Figure 6a) P1, (Figure 6b) P5, and (Figure 6c) P10. According to Figure 5, it can be observed that there is a discrepancy between the results based on the different reference points. For example, SSD based on P5 is overestimated in comparison P1 and P10.

Table 1 is presented to quantify the model performance and compare the statistical quantities of R^2, RMSE (m^3/s), PBIAS (%), MAE (m^3/s), and KGE based on 10 reference points (from P1 to P10) in the Gono River. The R^2 values are about 0.998 and the same for the

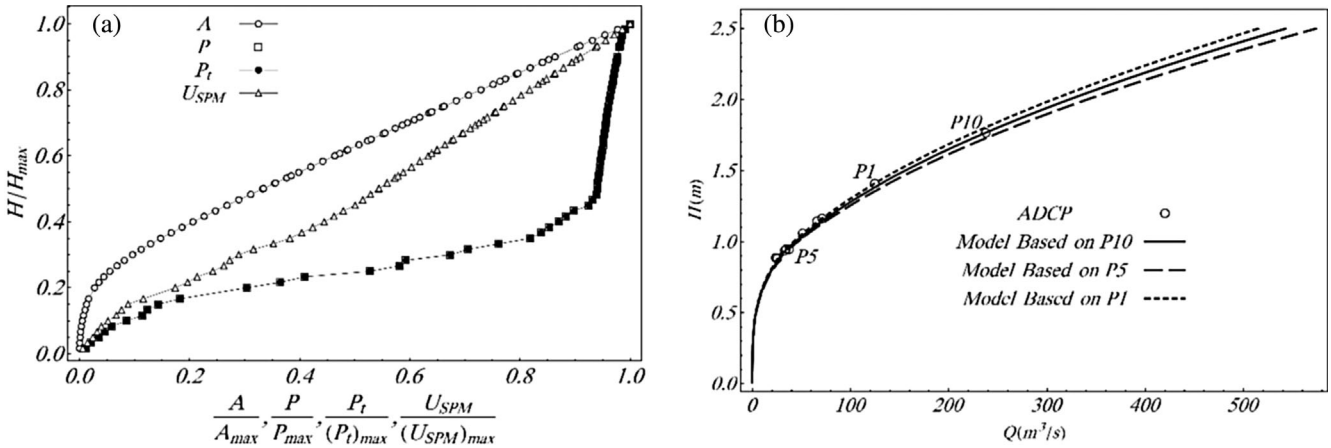

FIGURE 5 (a) Variation of the relative values of A, P, P_t, and U_{SPM}. (b) The single stage-discharge model based on three different reference points

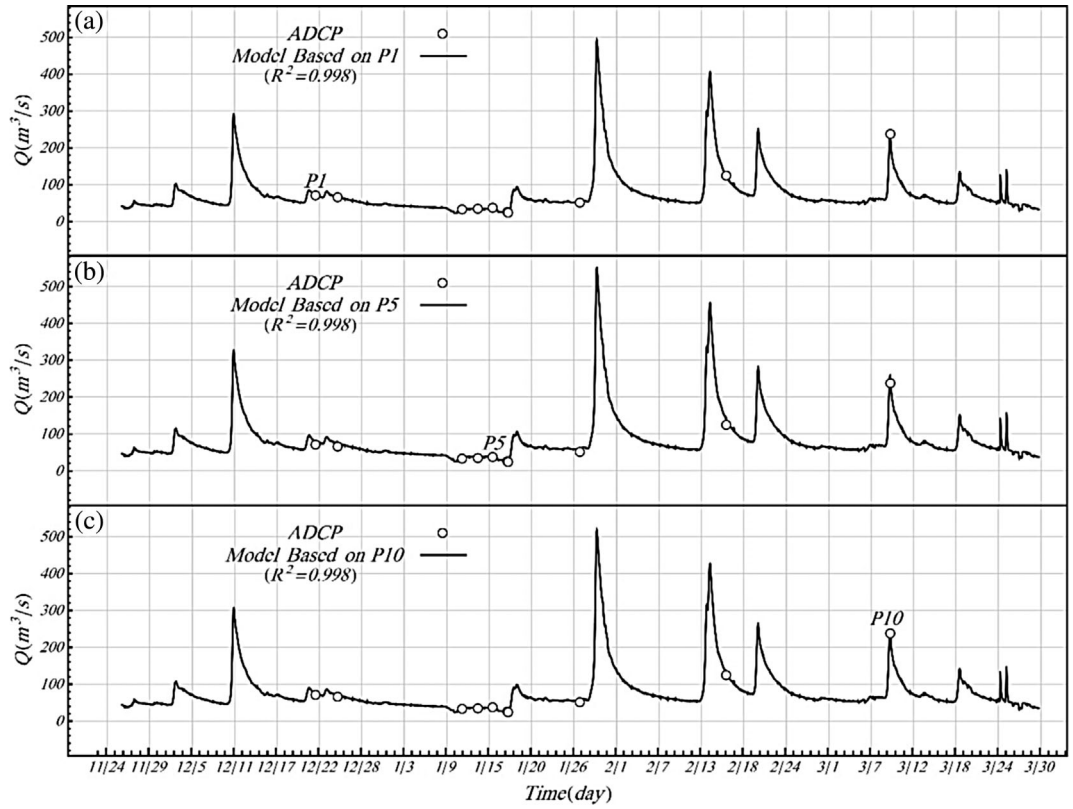

FIGURE 6 Hydrographs of measured and simulated flows using the single stage-discharge method based on (a) P1, (b) P5, and (c) P10 reference points in the Gono River

TABLE 1 The performance metrics results of the SSD method based on different reference points

Point	R^2	RMSE (m^3/s)	PBIAS (%)	MAE (m^3/s)	KGE
P1	0.998	3.91	−1.78	2.20	0.968
P2	0.998	5.63	−4.10	3.22	0.951
P3	0.998	2.81	0.98	2.32	0.971
P4	0.998	2.84	0.72	2.30	0.972
P5	0.998	8.84	10.13	7.14	0.895
P6	0.998	4.01	−1.93	2.21	0.967
P7	0.998	10.30	−9.50	6.70	0.901
P8	0.998	4.32	−2.38	2.33	0.964
P9	0.998	4.14	−2.13	2.24	0.966
P10	0.998	3.39	3.18	2.71	0.958

Abbreviations: KGE, Kling-Gupta efficiency; MAE, mean absolute error; PBIAS, percent bias; RMSE, root mean square error.

model based on all reference points. There is a range of 2.81 to 10.3 m^3/s for all RMSE values. When P7 was used as reference data for model estimation, the RMSE was highest. P7 has the lowest stage in the available observational data, and probably due to not considering the roughness of the bed, the estimation error has increased with the help of this observational data. Approximately −10 to 10 is the range of the PBIAS criterion, with negative values causing overestimation and positive values causing underestimation. The least positive value of this criterion is related to the SSD based on P4. Also, the model based on the P5 reference point shows the highest MAE, possibly due to measurement error. The lowest and highest MAE is 2.20 and 7.14 (m^3/s), respectively. Regarding the KGE criterion, it can be concluded that the model based on P4 has the best performance (KGE = 0.972), whereas the model based on P5 has the worst performance (KGE = 0.895).

Therefore, as seen in Table 1, the model estimation based on most observed data shows similar performance based on the different error criteria. The reference data, which probably has a measurement

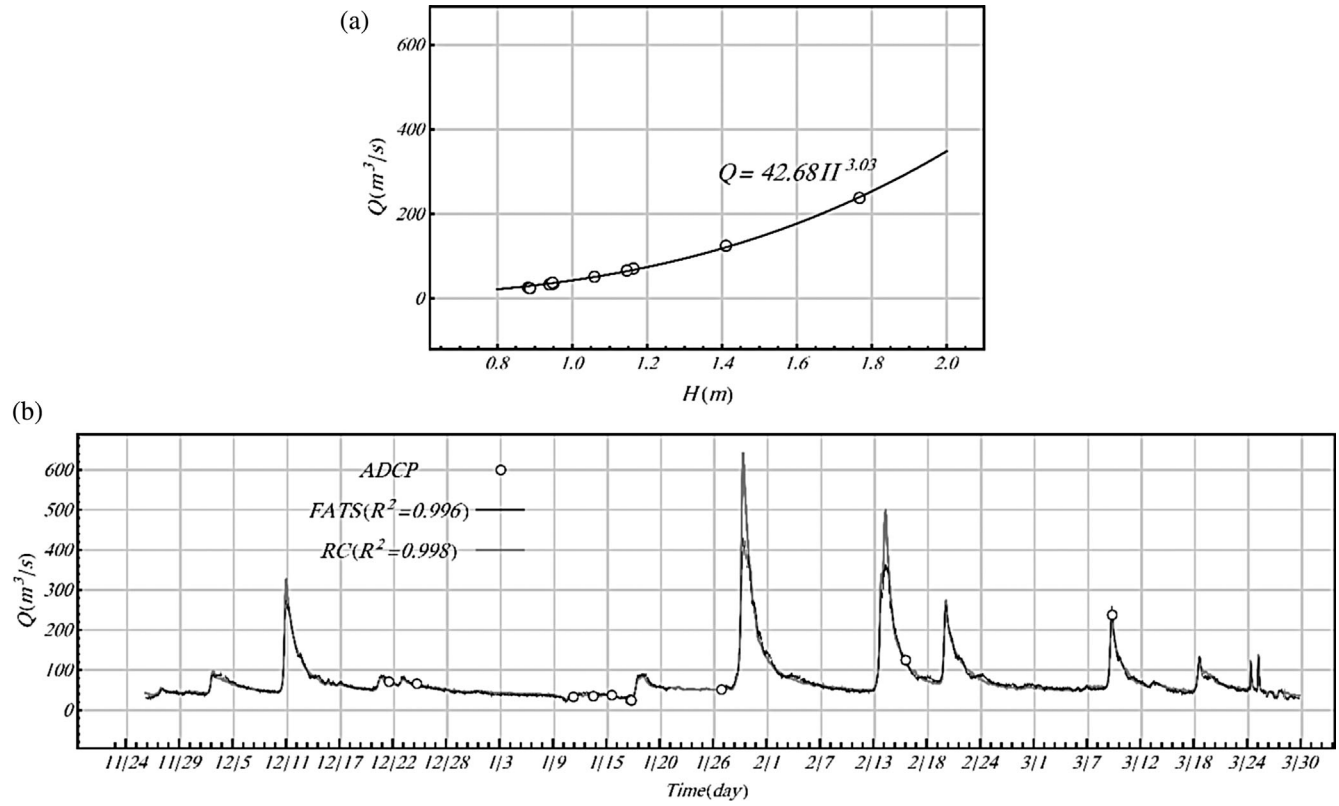

FIGURE 7 (a) Rating curve established by moving-boat acoustic Doppler current profiler measurements, and (b) time series of streamflow estimated by fluvial acoustic tomography system and rating curve

error or is near the river bed, causes more errors in the streamflow estimation.

3.2 | Results of previous studies

After studying the proposed model's performance, it is time to compare it with the previous studies that have been done. Two methods, FATS and RC, have been carried on in the Gono River.

Figure 7a shows the relationship between water depth (H) and the moving-boat ADCP discharge estimates. The power function of Equation (2) is fitted to all the available ADCP datasets to establish the RC. The R^2 value is 0.998, which indicates a proper performance.

FATS, RC, and ADCP are all used to measure temporal variations of streamflow in Figure 7b. The performance of both methods ($R^2 > 0.99$) is appropriate; however, the RC model is overestimated compared to the FATS. RC estimates peak discharge at 650 m^3/s, while FATS estimates 430 m^3/s.

3.3 | The application of the FARC in continuous streamflow

In this model, suitable curves must first be fitted between mean velocity-depth and wetted area-depth. According to observed data, the mean velocity-depth (Figure 8a) and wetted area-depth (Figure 8b) relation is selected from the power function (Manfreda et al., 2020). The R^2 value in both velocity-depth ($R^2 = 0.96$) and wetted area-depth ($R^2 = 0.99$) relation shows a robust linear relationship between the observed and estimated values. The product of the mean velocity-depth and the wetted area-depth functions leads to estimating the discharge and rating curve. The product of the mean velocity-depth and wetted area-depth functions leads to estimating the discharge. Figure 8c illustrates the continuous streamflow estimation by the FARC method. As can be seen, the model's performance is acceptable, and the R^2 value is about 0.998. The peak flow estimation by this model is about 660 m^3/s which is higher than RC.

3.4 | Model comparison and discussion

In order to quantify the error between FATS, RC, FARC, and SSD methods, a relative error is calculated in Table 2. The error is calculated with $([Q_e - Q_{ADCP}]/Q_{ADCP}) \times 100$. The estimated discharge (Q_e) of FATS, RC, and FARC methods is in Table A1. Also, the results of relative errors of the SSD model based on all reference points are in Table A2. In Table 2, just the SSD model based on P4 is mentioned.

As shown in Table 2, the maximum and minimum relative errors in the proposed model based on P4 are about 11 and −0.7%, respectively. It should be noted that the model error based on P4 in the

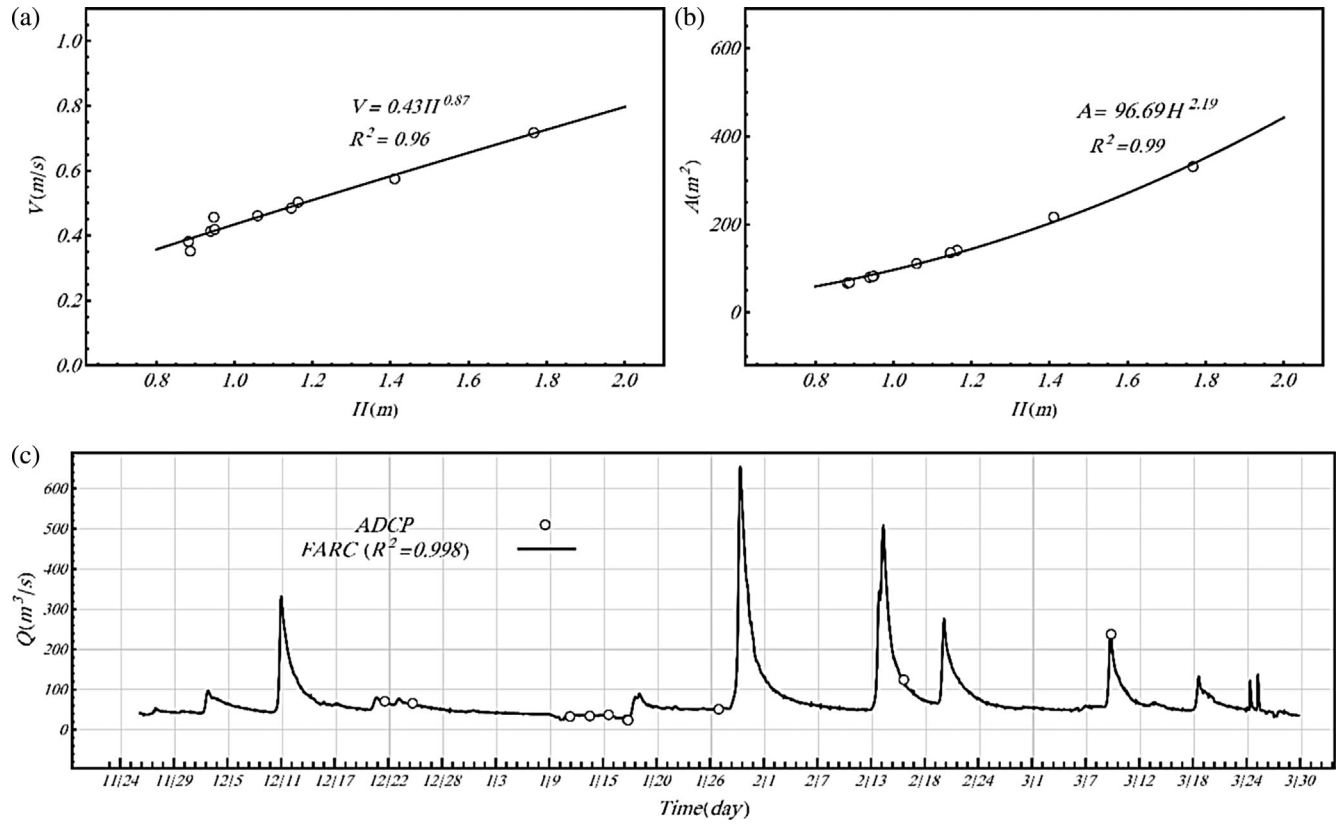

FIGURE 8 Fitted functions between (a) mean velocity-depth and (b) wetted area-depth; and (c) time series of streamflow estimated by flow-area rating curve

TABLE 2 Relative errors of FATS, RC, FARC, and SSD models

				Relative error (%)			
Point	Date	Time	Q_{ADCP} (m^3/s)	SSD based on P4	FATS	RC	FARC
1	December 22, 2015	13:00	70.96	2.59	−2.17	−4.90	−5.77
2	December 25, 2015	13:22	65.91	5.36	−0.68	−2.21	−2.92
3	January 11, 2016	12:45	33.10	−0.70	−11.68	6.58	4.32
4	January 13, 2016	16:20	34.60	–	11.33	5.40	3.40
5	January 15, 2016	16:45	37.46	−8.55	4.60	−3.33	−5.06
6	January 17, 2016	16:45	25.60	2.68	19.60	14.05	11.66
7	January 17, 2016	19:15	24.00	11.28	28.53	23.68	21.13
8	January 27, 2016	14:00	51.30	3.08	−8.45	−0.95	−2.34
9	February 16, 2016	13:10	124.67	2.97	4.39	−2.96	−3.06
10	March 9, 2016	22:10	237.63	−2.32	2.88	0.75	1.61

Abbreviations: ADCP, acoustic Doppler current profiler; FARC, flow-area rating curve; FATS, fluvial acoustic tomography system; RC, rating curve; SSD, single stage-discharge.

measured discharge data P4 is zero, so it is not considered. The maximum relative errors in FATS, RC, and FARC models are about 28, 24, and 21%, respectively, and the minimum ones are about −0.7, −0.95, and 1.61%, respectively.

The comparison of studied models based on five performance criteria is presented in Table 3. R^2 values for all studied models are greater than 0.996, indicating good performance based on this criterion. As can be seen in Table 3, the least RMSE and MAE are related to the SSD method; however, the lowest PBIAS is related to the flow-area method. Furthermore, the flow-area method outperforms other methods based on the KGE criterion. After that, RC shows the proper performance based on PBIAS and KGE indices. The FATS is not shown proper performance compared to other models.

TABLE 3 Comparison of different models for streamflow estimation

Model	R^2	RMSE (m^3/s)	PBIAS (%)	MAE (m^3/s)	KGE
SSD based on P4	0.998	2.838	0.715	2.30	0.972
FATS	0.996	4.512	2.784	4.00	0.972
RC	0.998	2.937	0.674	2.55	0.982
FARC	0.998	3.044	0.221	2.74	0.997

Abbreviations: FARC, flow-area rating curve; FATS, fluvial acoustic tomography system; KGE, Kling-Gupta efficiency; MAE, mean absolute error; PBIAS, percent bias; RC, rating curve; RMSE, root mean square error; SSD, single stage-discharge.

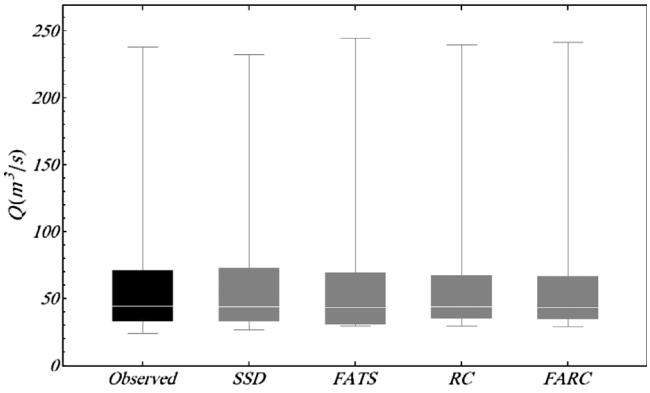

FIGURE 9 The box plot displays the observed and estimated discharge distribution for the four models

The box plot of the observed and estimated discharge is depicted in Figure 9. The RC model captured the extreme values better than the other models. However, all the studied models demonstrated a more remarkable ability to capture the peak discharge values. The FATS method showed the least efficacy in estimating high values.

For evaluating the best estimate with the least data, it is assumed that observations are not available higher than 1 m from the riverbed. Therefore, they should not be used as calibration. Rating curve models are tested using observational data higher than 1 m from the riverbed. As a result, five observational data are used as calibrations, and five are used as testing. The percentage of relative error in the test step is presented in Table 4. Calibration is carried out at observation points P3 to P7 since they are all below the $H = 1$ m, and the other points are used for tests. It can be seen that the SSD model shows an excellent performance than the other two models. As the stage increases, the relative error of the RC and FARC increases and reaches the maximum values of 287 and 281%, respectively. However, the maximum estimation error based on the SSD method equals 5.36%.

The performance of the upper assumption results is presented in Table 5. As can be seen, the RC and FARC methods are susceptible to the number of observation data and show a significant error. In contrast, there is no change in the results of the proposed method compared to the previous state.

Therefore, the three studied methods for estimating the rating curve are acceptable if sufficient observational data is available at the lower and upper levels. However, when observational data is available only from lower stages, discharge estimation with two methods is subject to a lot of error. Despite this, SSD has no sensitivity. Consequently, this method can provide a reasonable discharge estimate even in areas with scarce data and only using lower-stage data.

4 | CONCLUSIONS

Accurate streamflow estimation is necessary for efficient water management and hydrological modeling. This study evaluated the proposed model rating curve (SSD model) to estimate streamflow based on only one observed data in the Gono River. The comparative results of the SSD model, FATS, RC, and FARC models' potential to estimate the streamflow were investigated. To examine the performance of the proposed model, some statistical measures, including the R^2, RMSE, PBIAS, MAE, and KGE criteria, are used. Overall, according to three statistical measures, the SSD model estimation based on all reference points is excellent and acceptable. The evaluation of the model performance revealed that the SSD method outperformed the FATS for estimating the streamflow of the Gono River. The SSD method is comparable to RC and FARC if all observed data is used for calibration. However, if the number of observation data for calibration is reduced (observations that the stage is less than 1 m), the performance of RC and FARC methods significantly reduces compared to the SSD method. Therefore, in the SSD method, observation data at lower levels are sufficient for proper flow estimation. While in the other two methods, it is necessary to have observational data at higher levels.

The presentation of the performance of the new relationship shows that the proposed expression has an appropriate capability in estimating continuous streamflow. The most significant advantage of the proposed method is its practicality in deprived areas where there is not enough measured data. Therefore, this method can assist managers in improving the robustness of water management decisions and research in hydrology in regions with few gauging for calibration.

This research can be developed by considering the heterogeneous roughness coefficient because the effect of bed roughness is not considered in this study. Moreover, the proposed model does not consider the unsteady conditions of the flow, so its effects can be considered a continuation of the current paper. Geometrical data in this research were derived from field measurements, so using remote sensing data instead of them creates a new approach to the research.

TABLE 4 Relative errors of RC, FARC, and SSD models in the testing step by considering five observed points for calibration

Point	Date	Time	Q_{ADCP} (m^3/s)	Relative error (%)		
				SSD based on P4	RC	FARC
1	December 22, 2015	13:00	70.96	2.59	46	45
2	December 25, 2015	13:22	65.91	5.36	45	45
8	January 27, 2016	14:00	51.30	3.08	23	23
9	February 16, 2016	13:10	124.67	2.97	127	125
10	March 9, 2016	22:10	237.63	−2.32	287	281

Abbreviations: ADCP, acoustic Doppler current profiler; FARC, flow-area rating curve; RC, rating curve; SSD, single stage-discharge.

TABLE 5 Comparison of rating curve models for streamflow estimation by considering five observed points for calibration

Model	R^2	RMSE (m^3/s)	PBIAS (%)	MAE (m^3/s)	KGE
SSD based on P4	0.998	2.838	0.715	2.30	0.972
RC	0.960	222	130	92.17	−0.540
FARC	0.960	218	128	90.60	−0.517

Abbreviations: FARC, flow-area rating curve; KGE, Kling-Gupta efficiency; MAE, mean absolute error; PBIAS, percent bias; RC, rating curve; RMSE, root mean square error; SSD, single stage-discharge.

In future research, it might be a good idea to use machine learning methods rather than the proposed model considering hydraulic and geometric parameters.

DATA AVAILABILITY STATEMENT

The following data used during the study for the Gono River are available upon request from the corresponding author: continuous streamflow measurement; water level data; cross-section data. Furthermore, all codes generated during the study are available upon request from the corresponding author.

ORCID

Mahmoud F. Maghrebi https://orcid.org/0000-0002-0082-0020

REFERENCES

Ajmera, T. K., & Goyal, M. K. (2012). Development of stage-discharge rating curve using model tree and neural networks: An application to Peachtree Creek in Atlanta. *Expert Systems with Applications*, *39*(5), 5702–5710. https://doi.org/10.1016/j.eswa.2011.11.101

Al Sawaf, M. B., Kawanisi, K., Kagami, J., Bahreinimotlagh, M., & Danial, M. M. (2017). Scaling characteristics of mountainous river flow fluctuations determined using a shallow-water acoustic tomography system. *Physica A: Statistical Mechanics and its Applications*, *484*, 11–20. https://doi.org/10.1016/j.physa.2017.04.168

Bhattacharya, B., & Solomatine, D. P. (2000). *Application of artificial neural network in stage-discharge relationship*. Proceedings of the 4th International Conference on Hydroinformatics.

Cheng, Z., Lee, K., Kim, D., Muste, M., Vidmar, P., & Hulme, J. (2019). Experimental evidence on the performance of rating curves for continuous discharge estimation in complex flow situations. *Journal of Hydrology*, *568*, 959–971. https://doi.org/10.1016/j.jhydrol.2018.11.021

Chicco, D., Warrens, M. J., & Jurman, G. (2021). The coefficient of determination R-squared is more informative than SMAPE, MAE, MAPE, MSE and RMSE in regression analysis evaluation. *PeerJ Computer Science*, *7*, e623. https://doi.org/10.7717/PEERJ-CS.623

Clarke, R. T. (1999). Uncertainty in the estimation of mean annual flood due to rating curve definition. *Journal of Hydrology*, *222*, 185–190.

Deka, P., & Chandramouli, V. (2003). A fuzzy neural network model for deriving the river stage-discharge relationship. *Hydrological Sciences Journal*, *48*(2), 197–209. https://doi.org/10.1623/hysj.48.2.197.44697

Di Baldassarre, G., & Montanari, A. (2009). Uncertainty in river discharge observations: A quantitative analysis. *Hydrology and Earth System Sciences*, *13*(6), 913–921. https://doi.org/10.5194/hess-13-913-2009

Elbeltagi, A., Kumar, M., Kushwaha, N. L., Pande, C. B., Ditthakit, P., Vishwakarma, D. K., & Subeesh, A. (2022). Drought indicator analysis and forecasting using data driven models: Case study in Jaisalmer, India. *Stochastic Environmental Research and Risk Assessment*, 1–19. https://doi.org/10.1007/s00477-022-02277-0

Farsoudeh, M., & Maghrebi, M. F. (2018). Impact of mean velocity accuracy on the estimation of rating curves in compound channels. *Flow Measurement and Instrumentation*, *64*, 242–251. https://doi.org/10.1016/j.flowmeasinst.2018.10.026

Ghorbani, M. A., Khatibi, R., Goel, A., FazeliFard, M. H., & Azani, A. (2016). Modeling river discharge time series using support vector machine and artificial neural networks. *Environmental Earth Sciences*, *75*(8), 685. https://doi.org/10.1007/s12665-016-5435-6

Gordon, R. L. (1989). Acoustic measurement of river discharge. *Journal of Hydraulic Engineering*, *115*(7), 925–936.

Gupta, H. V., Kling, H., Yilmaz, K. K., & Martinez, G. F. (2009). Decomposition of the mean squared error and NSE performance criteria: Implications for improving hydrological modelling. *Journal of Hydrology*, *377*(1–2), 80–91.

Gupta, H. V., Sorooshian, S., & Yapo, P. O. (1999). Status of automatic calibration for hydrologic models: Comparison with multilevel expert calibration. *Journal of Hydrologic Engineering*, *4*(2), 135–143.

Herschy, R. W. (2009). Streamflow measurement. *Environmental & Engineering Geoscience*, *2*, 609–610. https://doi.org/10.2113/gseegeosci.ii.4.609

Kawanisi, K., Al Sawaf, M. B., & Danial, M. M. (2018). Automated real-time stream flow acquisition in a mountainous river using acoustic tomography. *Journal of Hydrologic Engineering*, *23*(2), 1–7. https://doi.org/10.1061/(ASCE)HE.1943-5584.0001604

Kawanisi, K., Bahrainimotlagh, M., Al Sawaf, M. B., & Razaz, M. (2016). High-frequency streamflow acquisition and bed level/flow angle estimates in a mountainous river using shallow-water acoustic tomography. *Hydrological Processes*, *30*(13), 2247–2254. https://doi.org/10.1002/hyp.10796

Kawanisi, K., Razaz, M., Ishikawa, K., Yano, J., & Soltaniasl, M. (2012). Continuous measurements of flow rate in a shallow gravel-bed river by a new acoustic system. *Water Resources Research*, *48*(5), 1–10. https://doi.org/10.1029/2012WR012064

Knoben, W. J. M., Freer, J. E., & Woods, R. A. (2019). Technical note: Inherent benchmark or not? Comparing Nash-Sutcliffe and Kling-Gupta efficiency scores. *Hydrology and Earth System Sciences*, *23*(10), 4323–4331. https://doi.org/10.5194/hess-23-4323-2019

Le Coz, J., Pierrefeu, G., & Paquier, A. (2008). Evaluation of river discharges monitored by a fixed side-looking Doppler profiler. *Water Resources Research*, *46*(4), 1–13. https://doi.org/10.1029/2008WR006967

Liu, D. (2020). A rational performance criterion for hydrological model. *Journal of Hydrology*, *590*, 125488. https://doi.org/10.1016/j.jhydrol.2020.125488

Maghrebi, M. F. (2006). Application of the single point measurement in discharge estimation. *Advances in Water Resources*, *29*(10), 1504–1514. https://doi.org/10.1016/j.advwatres.2005.11.007

Maghrebi, M. F., Ahmadi, A., Attari, M., & Maghrebi, R. F. (2016). New method for estimation of stage-discharge curves in natural rivers. *Flow Measurement and Instrumentation*, *52*, 67–76. https://doi.org/10.1016/j.flowmeasinst.2016.09.008

Maghrebi, M. F., & Ball, J. E. (2006). New method for estimation of discharge. *Journal of Hydraulic Engineering*, *132*(10), 1044–1051. https://doi.org/10.1061/(ASCE)0733-9429(2006)132:10(1044)

Manfreda, S. (2018). On the derivation of flow rating curves in data-scarce environments. *Journal of Hydrology*, *562*, 151–154. https://doi.org/10.1016/j.jhydrol.2018.04.058

Manfreda, S., Pizarro, A., Moramarco, T., Cimorelli, L., Pianese, D., & Barbetta, S. (2020). Potential advantages of flow-area rating curves compared to classic stage-discharge-relations. *Journal of Hydrology*, *585*, 124752. https://doi.org/10.1016/j.jhydrol.2020.124752

Muste, M., Ho, H. C., & Kim, D. (2011). Considerations on direct stream flow measurements using video imagery: Outlook and research needs. *Journal of Hydro-Environment Research*, *5*(4), 289–300. https://doi.org/10.1016/j.jher.2010.11.002

Ocio, D., Le Vine, N., Westerberg, I., Pappenberger, F., & Buytaert, W. (2017). The role of rating curve uncertainty in real-time flood forecasting. *Water Resources Research*, *53*(5), 4197–4213.

Razaz, M., Kawanisi, K., Kaneko, A., & Nistor, I. (2015). Application of acoustic tomography to reconstruct the horizontal flow velocity field in a shallow river. *Water Resources Research*, *51*(12), 9665–9678.

Shukla, R., Kumar, P., Vishwakarma, D. K., Ali, R., Kumar, R., & Kuriqi, A. (2022). Modeling of stage-discharge using back propagation ANN-, ANFIS-, and WANN-based computing techniques. *Theoretical and Applied Climatology*, *147*(3–4), 867–889. https://doi.org/10.1007/s00704-021-03863-y

Singh, A. K., Kumar, P., Ali, R., Al-Ansari, N., Vishwakarma, D. K., Kushwaha, K. S., … Heddam, S. (2022). An integrated statistical-machine learning approach for runoff prediction. *Sustainability*, *14*(13), 8209. https://doi.org/10.3390/su14138209

Sivapragasam, C., & Muttil, N. (2005). Discharge rating curve extension - a new approach. *Water Resources Management*, *19*(5), 505–520. https://doi.org/10.1007/s11269-005-6811-2

Vatanchi, S. M., & Maghrebi, M. F. (2019). Uncertainty in rating-curves due to manning roughness coefficient. *Water Resources Management*, *33*(15), 5153–5167. https://doi.org/10.1007/s11269-019-02421-6

Vishwakarma, D. K., Pandey, K., Kaur, A., Kushwaha, N. L., Kumar, R., Ali, R., … Kuriqi, A. (2022). Methods to estimate evapotranspiration in humid and subtropical climate conditions. *Agricultural Water Management*, *261*, 107378. https://doi.org/10.1016/j.agwat.2021.107378

How to cite this article: Maghrebi, M. F., Vatanchi, S. M., & Kawanisi, K. (2023). Investigation of stage-discharge model performance for streamflow estimating: A case study of the Gono River, Japan. *River Research and Applications*, 1–14. https://doi.org/10.1002/rra.4106

APPENDIX A

TABLE A1 Estimated discharges of ADCP, FATS, RC, and FARC

Point	Date	Time	Q_{ADCP} (m^3/s)	Q_{FATS} (m^3/s)	Q_{RC} (m^3/s)	Q_{FARC} (m^3/s)
1	December 22, 2015	13:00	70.96	69.42	71.76	66.87
2	December 25, 2015	13:22	65.91	65.46	67.50	63.99
3	January 11, 2016	12:45	33.10	29.24	32.12	34.53
4	January 13, 2016	16:20	34.60	38.52	33.88	35.77
5	January 15, 2016	16:45	37.46	39.18	33.44	35.56
6	January 17, 2016	16:45	25.60	30.61	24.65	28.58
7	January 17, 2016	19:15	24.00	30.85	25.84	29.07
8	January 27, 2016	14:00	51.30	46.96	51.59	50.10
9	February 16, 2016	13:10	124.67	130.14	127.01	120.86
10	March 9, 2016	22:10	237.63	244.48	220.27	241.45

TABLE A2 Relative errors of SSD method based on different reference points

	Relative error of SSD based on									
Q_{ADCP} (m^3/s)	P1	P2	P3	P4	P5	P6	P7	P8	P9	P10
70.96	–	−2.31	2.86	2.59	12.18	−0.10	−7.8	−0.50	−0.31	5.1
65.91	2.75	–	5.63	5.36	15.2	2.59	−5.3	2.12	2.38	7.94
33.10	−3.16	−5.45	–	−0.70	8.6	−3.3	−10.8	−3.71	−3.5	1.73
34.60	−2.64	−4.94	0.09	–	9.17	−2.78	−10.3	−3.20	−2.98	2.28
37.46	−10.8	−12.92	−8.31	−8.55	–	−10.9	−17.8	−11.3	−11.1	−6.31
25.60	0.13	−2.23	2.95	2.68	12.27	–	−7.7	−0.47	−0.22	5.19
24.00	8.53	5.96	11.6	11.28	21.69	8.36	–	7.90	8.14	14.00
51.30	0.53	−1.85	3.35	3.08	12.72	0.38	−7.4	–	0.17	5.61
124.67	0.42	−1.96	3.23	2.97	12.59	0.27	−7.5	−0.21	–	5.49
237.63	−4.74	−6.7	−2.06	−2.32	6.81	−4.88	−12.2	−5.32	−5.08	–